British Journal of Pharmacology

DOI:10.1111/j.1476-5381.2011.01356.x
www.brjpharmacol.org

RESEARCH PAPER

Preserved arterial vasodilatation via endothelial protease-activated receptor-2 in obese type 2 diabetic mice

Satomi Kagota, Elizabeth Chia and John J McGuire

Cardiovascular Research Group, Division of BioMedical Sciences, Memorial University, St. John's, Newfoundland and Labrador, Canada

Correspondence
Satomi Kagota, Department of Pharmacology, School of Pharmaceutical Sciences, Mukogawa Women's University, 11-68 Koshien Kyuban-cho, Nishinomiya 663-8179, Japan.
E-mail: skagota@mukogawa-u.ac.jp

Keywords
endothelial dysfunction; obesity; diabetes; protease-activated receptors; resistance arteries; nitric oxide

Received
26 August 2010
Revised
2 February 2011
Accepted
26 February 2011

BACKGROUND AND PURPOSE

In non-obese diabetic animals, protease-activated receptor-2 (PAR2) agonists are more effective vasodilators, which is attributed to increased COX-2 and endothelial NOS (eNOS) activities. Under conditions of diabetes and obesity, the effectiveness of PAR2 agonists is unknown. We compared the vasodilator responses of small calibre mesenteric arteries from obese diabetic B6.BKS(D)-*Lepr*^{db}/J (db/db) induced by PAR2-activating agonists 2-furoyl-LIGRLO-amide (2fly) and trypsin to those obtained in controls [C57BL/6J (C57)], and assessed the contributions of COX, NOS and calcium-activated potassium channels (K_{Ca}) to these responses.

EXPERIMENTAL APPROACH

Arteries mounted in wire myographs under isometric tension conditions were contracted submaximally by U46619 then exposed to vasodilators. mRNA and protein expression of PAR2, eNOS and soluble GC (sGC) were determined by real-time PCR and Western blots.

KEY RESULTS

ACh- and nitroprusside-induced relaxations were attenuated in db/db compared with C57. In contrast, 2fly- and trypsin-induced relaxations were largely retained in db/db. A NOS inhibitor partly inhibited ACh- and 2fly-induced relaxations in C57, but not those in db/db. Inhibitors of the COX-cAMP pathway (FR122044, SC560, NS398, SC58125, SQ22536, CAY10441) did not affect these relaxation responses in either strain. Charybdotoxin (BK_{Ca}, SK3.1 blocker), but not iberiotoxin (BK_{Ca} blocker), inhibited responses to the PAR2 agonists in db/db. In db/db protein levels of eNOS were higher, whereas those of sGC were lower than in C57. PAR2 mRNA expression in db/db was higher than in C57.

CONCLUSIONS AND IMPLICATIONS

PAR2-mediated vasodilatation is protected against the negative effects of obesity and diabetes in mice. In diabetic vascular dysfunction, preserved PAR2 vasodilatation was linked to activation of SK3.1.

Abbreviations

2fly, 2-furoyl-LIGRLO-amide; BK_{Ca}, large (big) conductance K_{Ca}; ChTx, charybdotoxin; CRC, concentration–response curve; eNOS, endothelial NOS; IbTx, iberiotoxin ; K_{Ca}, Ca^{2+}-activated potassium channel; L-NAME, N^G-nitro-L-arginine methyl ester; PAR2. protease-activated receptor 2; SK2.2/2.3, small-conductance K_{Ca}; SK3.1, intermediate-conductance $K_{Ca;}$ sGC, soluble GC

Introduction

The endothelium of blood vessels expresses protease-activated receptor-2 (PAR2), one of four types of protease-activated seven transmembrane G protein-coupled receptors (Ramachandran and Hollenberg, 2008). Various identified serine proteinases cleave a specific recognition site in the extracellular N-terminus of PAR2 to unmask a hidden sequence that then functions as a tethered ligand to activate the receptor while other proteases disarm the receptor (Hansen *et al*., 2008). PAR2 expression is found under normal conditions on many epitheliums, nociceptive neuron terminals, dorsal root ganglion bodies and glial cells. Thus, studies have implicated a role for PAR2 in many disease conditions including inflammation responses in cardiovascular, respiratory, gastrointestinal and nervous systems (Hansen *et al*., 2008; Ramachandran and Hollenberg, 2008). With a few exceptions, the consensus from the results of these studies is that the role of PAR2 is to provide small inputs to modulate disease and injury responses in experimental models. For example, PAR2 gene deletion produces a haemodynamic phenotype characterized by modest (5%) elevation of systolic blood pressures in conscious mice (McGuire *et al*., 2007). Human diseases are complex phenotypes involving multiple organ systems, thus the role of PAR2 still needs to be pursued in many experimental models.

Humans with metabolic syndrome, which is a controversial definition of health status characterized by the clustering of multiple cardiovascular risk factors such as abdominal obesity, insulin resistance and hypertension, are known to be at higher risk of developing vascular diseases (Shaw *et al*., 2005; Venkatapuram and Shannon, 2006). Increased PAR2 immunoreactivity has been reported in samples from human coronary atherosclerotic lesions (Napoli *et al*., 2004) and in rat carotid arteries after experimental angioplasty balloon-injury (Damiano *et al*., 1999). Direct exposure to inflammatory substances, TNF-α and IL-1α, was reported to induce PAR2 expression in endothelium from human arteries *in vitro* (Hamilton *et al*., 2001). However, the functional consequences, specifically for PAR2-mediated endothelium-dependent responses, such as vasodilatation, in these disease conditions are not fully understood. In rodent models of hypertension, we and others have reported that PAR2-mediated relaxation persists in resistance arteries despite dysfunctional responses to other endothelium-dependent agonists (Sobey and Cocks, 1998; McGuire *et al*., 2007; Smeda and McGuire, 2007; Smeda *et al*., 2010). In diabetes models, the sensitivity to PAR2-mediated relaxation was increased in aortae from type 1 non-obese diabetic (NOD) mice (Roviezzo *et al*., 2005) and in mesenteric arteries from type 2 non-obese diabetic rats (Goto-Kakizaki) (Matsumoto *et al*., 2009). In these models, PAR2-mediated vasodilatation of large calibre arteries was dependent on the up-regulation of either COX or NOS. However, the mechanism of PAR2-mediated endothelium-dependent responses in obese type 2 diabetes models is not known.

The main objective of this study was to investigate vascular responses, especially those mediated by PAR2, in mesenteric arteries of obese type 2 diabetic B6.BKS(D)-*Lepr*^{db}/J mice (db/db). A mutation of the leptin receptor in these mice causes a lack of leptin receptor signalling in their hypothalamus, which leads to overeating, obesity, hyperglycaemia and hyperlipidaemia in these mice, which is similar to human type 2 diabetes and metabolic syndrome (Russell and Proctor, 2006; Kennedy *et al*. 2010). To date, db/db have been widely used in studies that have evaluated diabetic complications, including the dysfunction of vasodilatation mechanisms in type 2 diabetes (Pannirselvam *et al*., 2002; Guo *et al*. 2005; Belmadani *et al*. 2008; Miike *et al*., 2008; Park *et al*., 2008). In this study, we found that the PAR2-mediated relaxations in second order mesenteric arteries of obese type 2 diabetic db/db were maintained while responses to ACh were attenuated; this was attributed to altered protein levels of sGC and eNOS. Neither COX-AC nor NO-sGC signalling appear to be involved in these PAR2-mediated responses in db/db mice. However, the mechanism of the preserved PAR2-mediated vasodilatation was linked to calcium-activated potassium channels (K_{Ca}), particularly SK3.1.

Methods

Animals

Male homozygous mice for the diabetes spontaneous mutation in leptin receptor [B6.BKS(D)-*Lepr*^{db}/J (db/db; stock #697; July 2009-October 2010)] and age-matched genetic background C57BL/6J (C57) (stock #664) mice were purchased from the Jackson Laboratory (Bar Harbor, ME, USA). Mice were fed a standard regular salt feed (NIH-31 autoclavable open formula mouse diet; Zeigler Bros Inc., Gardners, PA, USA) and provided water *ad libitum* while housed in the Animal Care Facility. All protocols were approved by the Institutional Animal Care Committee of Memorial University in accordance with the guidelines and principles for use of animals in research by the Canadian Council on Animal Care. Mice (12 weeks of age), were anaesthetized with isoflurane for cardiac puncture to obtain blood samples and then killed by cervical dislocation.

Sources of drugs and reagents for myograph studies

Unless stated otherwise, all drugs and reagents were obtained from Sigma Aldrich (Oakville, Ontario, Canada). Other sources included: Bachem (Torrance, CA, USA), charybdotoxin; Cayman Chemicals (Ann Arbor, MI, USA), CAY10441, SC560, SC58125 and SQ22536; Peptides International (Louisville, KT, USA), 2-furoyl-leu-ile-gly-arg-leu-orn-amide (2fly); Tocris BioScience (Ellisville, MO, USA): charybdotoxin (ChTx), FR122047, NS398; and University of Calgary Peptide Synthesis (Calgary, Alberta, Canada), 2-furoyl-orn-leu-arg-gly-ile-leu-amide. Stock solutions of indomethacin, FR122047, CAY10441, NS398, SC560, SC58125 and SQ22536 were made up in dimethylsulphoxide and added as a 1/1000 dilution to tissue bath solutions. Stock solutions of all other drugs were made in water.

Vascular reactivity

Mesenteric arcades with attached adipose, blood vessels and nerves were dissected free from gastrointestinal tract *in situ* and immediately placed in ice-cooled Krebs buffered bicarbonate solution (114 mM NaCl, 4.7 mM KCl, 0.8 mM KH_2PO_4, 1.2 mM $MgCl_2$, 2.5 mM, $CaCl_2$, 25 mM $NaHCO_3$ and

11 mM D-glucose). Branches of second order mesenteric arteries were cleaned of adherent tissue and cut into 1–2 mm lengths. The arterial rings were positioned in small wire myograph chambers (DMT 610M, DMT 620M) for the measurement and recording of isometric tension (McGuire *et al.*, 2007). Each chamber contained Krebs buffered solution (pH 7.4) bubbled with 95% O_2/5% CO_2 at 37°C. Initial resting tension for each artery was determined as described previously (McGuire *et al.*, 2007), with initial effective pressure at 7.98 kPa. After an equilibration period (1 h), vascular reactivity was measured. Contractile responses were determined from cumulative additions of potassium chloride (15–120 mM), 9,11-dideoxy-9a,11a-methanoepoxy $PGF_{2\alpha}$ (U46619, 0.1 nM–3 μM) or phenylephrine (0.01–100 μM) to the baths. To determine the relaxation response, the rings were contracted by addition of small increments of U46619 to submaximal tensions [50–80% of E_{max} based on concentration–response curves (CRC) data]. After a stable contraction was obtained, a PAR2-activating peptide, 2fly (0.1 nM–3 μM), ACh (0.1 nM–100 μM) or nitroprusside (0.1 nM–100 μM) was added cumulatively to the bath. The contraction and relaxation responses were measured in either the absence or presence of inhibitors (30 min), which included N^G-nitro-L-arginine methyl ester (L-NAME, NOS inhibitor, 100 μM), FR122047 (selective COX-1 inhibitor, 3 μM), SC560 (selective COX-1 inhibitor, 3 μM), NS398 (selective COX-2 inhibitor, 3 μM), SC58125 (selective COX-2 inhibitor, 10 μM), SQ22536 (AC inhibitor, 100 μM), CAY10441 (PGI_2 receptor antagonist, 0.3 μM), apamin (SK2.2/2.3 inhibitor, 1 μM), ChTx (SK3.1/BK_{Ca} inhibitor, 50 nM) and iberiotoxin (BK_{Ca} inhibitor, 50 nM, IbTx). Inhibitor treatment with these antagonists were reported as being effective (Guo *et al.*, 2005; Roviezzo *et al.* 2005; Cao *et al.* 2006; Yamada *et al.*, 2008). In the experiments examining the removal of endothelium, the negative control reversed sequence PAR2-peptide (2-furoyl-OLRGIL-amide, 10 μM), trypsin (15 $U \cdot mL^{-1}$ = 30 nM; type IX-S porcine pancreas, 13 100 $U \cdot mg^{-1}$) and the inhibition of K_{Ca}, rings were contracted by U46619 as described above, then test compounds including ACh (10 μM) and 2fly (1 μM) were added at a single maximal effective concentration. The exception was the negative control peptide that was added at 10-times the maximal effective concentration of 2fly. Endothelium was damaged by passing a human hair through the lumen of an artery ring and was confirmed by absence of relaxation to ACh in the experiments.

Protein expression in whole mesenteric arteries

Western blots were performed on mesenteric arteries homogenized in lysis buffer [1% NP-40, 10% glycerol, 1 mM NaF, 1 mM Na_3VO_4, 0.025% sodium dodecyl sulphate (SDS) and protease inhibitors] using a glass homogenizer. Protein concentration was determined using a BCA protein assay kit (Pierce Biotechnology, Inc., Rockford, IL, USA), then proteins (5–20 μg) were loaded onto gels, separated by SDS polyacrylamide gel electrophoresis (8%) and transferred onto polyvinylidine difluoride membranes. Each sample was assayed in duplicate at two protein levels. Membranes were incubated separately with antibodies against COX-1 (Cayman Chemicals), COX-2 (C-20, Santa Cruz Biotechnology, Inc., Santa Cruz, CA, USA), eNOS (BD Biosciences, Lexington, KY, USA), sGC β1 subunit (Abcam, Inc., Cambridge, MA, USA) and glyceraldehyde 3-phosphate dehydrogenase (GAPDH) (FL-335, Santa Cruz Biotechnology). Immunoreactive bands on membranes were recorded on X-ray film by chemiluminescence detection according to supplier (SuperSignal West Pico Thermo Fisher Scientific Inc., Rockford, IL, USA). Minor modifications to the above procedures were made to assay arterial protein with monoclonal anti-human PAR2 antibody SAM11 (Molino *et al.*, 1997; SC-13504, Santa Cruz Biotechnology) and can be found in Supporting Information. Target band intensities were quantified by Image J (National Institute of Health, Bethesda, MD, USA). The density for GAPDH bands from the same blots were used to normalize the target band for quantitative analyses. Representative immunoblots of experiments were repeated independently three times.

mRNA expression

mRNA expression was assayed using quantitative real-time PCR methods. Mesenteric arterial beds were isolated as described above then flash frozen by immersion in liquid nitrogen. Total RNA was extracted from frozen tissues and then purified using an RNeasy fibrous kit following manufacturer's instructions (Qiagen, Mississauga, Ontario, Canada). Real-time measurement of target gene expression was carried out using TaqMan RNA-to-CT 1-step kit accordingly on an ABI Prism 7000 light cycler (Applied Biosystems, Foster City, CA, USA). The amount of RNA used was optimized for each target gene primer-fluorescent probe set. Gene specific primer-probe sets were available commercially (Applied Biosystems, assay/product ID: PAR2, Mm00433160_m1; eNOS, Mm00435204_m1; sGC, Mm00516926_m1; GAPDH, 4352932E; β_2-microglobulin, Mm00437762_m1; calnexin, Mm00500330_m1). Refer to Supporting Information Table S1 for more specific details on the TaqMan gene expression assays selected. In some instances, to accommodate low individual yield of samples, RNA was pooled from two to three mice and each pooled set was treated as one independent sample. Each sample was measured in duplicate. A triad housekeeping gene expression approach (GAPDH, β_2-microglobulin, calnexin) was used for normalization of sample material, and the efficiencies for primer sets for each were included in all calculations.

Blood and urine levels of glucose and serum insulin

Blood was collected by cardiac puncture on the date of myograph experiments from each mouse while under isoflurane-induced anaesthesia. The non-fasted blood and urine glucose were determined using Elite glucometer (blood glucose test strips 3986B, Bayer HealthCare LLC., Mishawaka, IN, USA) and Chemistrips (10A, Roche Diagnostics, Quebec, Quebec, Canada). Serum was separated by centrifugation at 3000× *g* for 10 min at 4°C, and insulin levels were determined by using ELISA (ultra sensitive mouse insulin ELISA, Crystal Chem. Inc., Downers Grove, IL, USA).

Data analysis

For myograph studies, individual CRCs were analysed by nonlinear regression curve fitting of drug concentration-

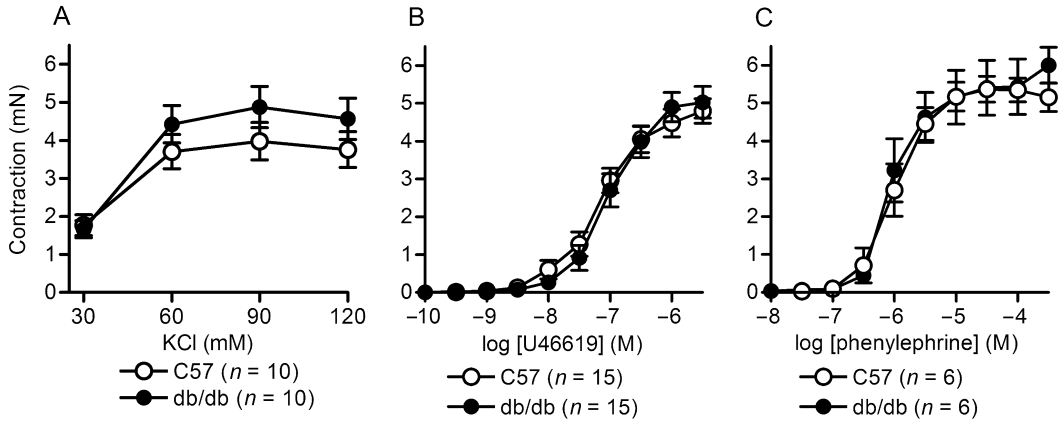

Figure 1

Extracellular K^+, U46619 and phenylephrine concentration-contraction response curves in db/db and C57BL/6J mesenteric arteries. Values are the mean ± SE (n = number of mice) for isometric tension changes to resting (untreated) baseline of isolated second order mesenteric arteries (2 mm lengths) after exposure to (A) various high K^+ solutions (isoosmotic balanced with Na^+), cumulative concentrations of (B) U46619 and (C) phenylephrine. There were no significant effects of strain on the responses to the drugs ($P > 0.05$, Student's t-test for unpaired data).

relaxation/contraction response relationships using a four parameter logistic function. We compared the negative log EC_{50} of the variables, Hill slope and E_{max} values between groups by Student's unpaired t test or two-way (strain × artery treatment) ANOVA as indicated in the legends of the Figures and Tables. In myograph studies that involved single concentrations of test compounds, comparisons of relaxations were determined by two-way or one-way ANOVA as indicated in the legends of the figures. Statistics indicating significant main effects or interactions were followed by Bonferroni *post hoc* for multiple comparison testing. $P < 0.05$ was considered significant. Myograph data are reported as mean ± SE, and n = number of mice. For protein expression data, target band density in each lane was normalized to the corresponding density for GAPDH. Protein, blood urine and serum data are reported as mean ± SE. Comparisons of variables between strains were made by Student's t-test for unpaired data. $P < 0.05$ was considered significant. In quantitative real-time PCR experiments, group-wise comparisons of relative expressions and statistical analyses of the relative expression results from real-time PCR were made using REST 2008 software (Pfaffl *et al.*, 2002) with data combined from three independent experimental runs. Data are reported as mean and SE interval for the ratio of db/db to C57 normalized target gene expression where n = number of independent samples. *$P < 0.05$ was considered significant.

Results

Metabolic phenotype of db/db mice

Body weights at 12 weeks of age of db/db (51.1 ± 0.6 g; n = 20) were about twofold heavier than age-matched control C57 (27.5 ± 0.5 g; n = 20; $P < 0.05$). Blood glucose levels of db/db were two times higher (22.9 ± 1.9 mmol·L^{-1}; n = 10) than C57 (11.1 ± 1.3 mmol·L^{-1}; n = 10; $P < 0.05$). Serum insulin levels of db/db were 30 times higher (34.1 ± 5.5 ng·mL^{-1}; n = 10) than C57 (1.13 ± 0.14 ng·mL^{-1}; n = 10; $P < 0.05$). Glucose was elevated (>55 mmol·L^{-1}) in urine from db/db, whereas in C57, it was at minimum detectable levels (<2 mmol·L^{-1}).

Vasoreactivity of second order mesenteric arteries from db/db mice

Contractions of mesenteric arteries induced by exposure to high K^+, U46619 and phenylephrine were not different between db/db and C57 (Figure 1).

Relaxations induced by the PAR2-activating peptide 2fly were preserved in db/db (Figure 2A, Table 1). On the other hand, ACh-induced relaxations of mesenteric arteries from db/db were attenuated compared with C57 (Figure 2B, Table 1). Damaging the endothelium of the arteries abolished the relaxations induced by both agonists in both strains [$P >$ 0.05, relaxation values were not different from 0, one sample t-test, C57 (n = 3 to 5); db/db (n = 6 to 7)]. A control peptide consisting of the reversed active amino acid sequence, 2-furoyl-OLRGIL-amide (10 μM), had no effect on either C57 (n = 6) or db/db (n = 6) arteries contracted by U46619 ($P >$ 0.05, relaxation values were not different from 0, one sample t-test).

Changes in NO-mediated relaxations in mesenteric arteries from db/db mice

To test the sensitivity of vascular smooth muscle cells to NO, nitroprusside (a NO donor)-induced relaxations were determined. The concentration–relaxation curve was significantly shifted to the right in db/db mice ($P < 0.05$, $-\log EC_{50}$ C57 vs db/db), but maximum responses were not significantly different between the two strains (Figure 2C and Table 1).

To test the contribution of eNOS activity to 2fly- and ACh-induced relaxations of U46619-contracted db/db mesenteric arteries, we obtained relaxation responses in the presence of an NOS inhibitor, L-NAME. L-NAME partly inhibited both the 2fly- and ACh-induced relaxations in C57 mice

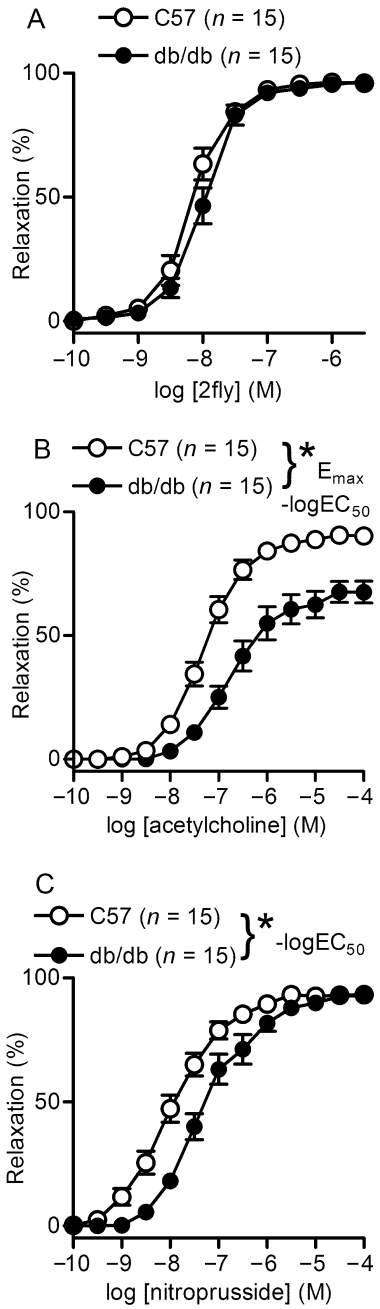

Figure 2

2-furoyl-LIGRLO-amide (2fly), ACh and nitroprusside concentration-relaxation response relationships of db/db and C57BL/6J (C57) mesenteric arteries. Values are the mean ± SE (n = number of mice) for (A) 2fly- (B) ACh- and (C) nitroprusside-induced relaxations of db/db and C57 second order mesenteric arteries contracted submaximally by U46619. 100% relaxation = complete reversal of contractions. *$P < 0.05$, db/db compared with C57 in (B) $-\log EC_{50}$ and E_{max} and (C) $-\log EC_{50}$, Student's t-test for unpaired data.

(Figure 3A and C; Table 2). However, it did not inhibit either of these responses in db/db mice (Figure 3B and D). In contrast, nitroprusside-induced relaxations were not inhibited by L-NAME in either strain of mice (Figure 3E and F).

To determine whether changes in the eNOS–sGC axis contributed to the lower sensitivity to NO, we assessed their protein expression in mesenteric arterial bed using the Western blot technique. Protein expression of eNOS was higher in db/db than in C57 mice, and sGC was lower in db/db than in the C57 strain (Figure 4).

Involvement of the COX pathway in PAR2-mediated relaxations in db/db mice

We determined the effects of selective COX-1 and COX-2 inhibitors on PAR2-mediated relaxations of mesenteric arteries to investigate the involvement of this pathway in the responses. COX-1-selective inhibitors, FR122047 and SC560, did not affect PAR2-mediated relaxations in either db/db or C57 mice (Figure 5A–D). Similar results were obtained for the COX-2 inhibitors, NS398 and SC58125 (Figure 5E–H). Furthermore, in agreement with the results obtained with the COX inhibitors, neither an AC inhibitor, SQ22536 nor a PGI_2 antagonist, CAY10441, inhibited the PAR2-mediated responses in either strain (Figure 6A–D). In addition, the protein expressions of COX-2 and COX-1 in the mesenteric arteries of db/db were not significantly different from those in the C57 mice (data not shown).

Contribution of K_{Ca} to PAR2-mediated relaxations in db/db mice

We determined the effects of BK_{Ca}, SK3.1, SK2.2 and SK2.3 inhibitors on PAR2-mediated relaxations of mesenteric arteries in db/db mice to investigate the contributions of K_{Ca} to these responses (Figure 7). In the presence of L-NAME, a combination of apamin (SK2.2 and SK2.3 inhibitor) plus ChTx (BK_{Ca} and SK3.1 inhibitor) abolished the ACh- and 2fly-induced relaxations in both C57 and db/db arteries (Figure 7A and B). To broaden the scope of our study of PAR2 agonists in db/db, we tested enzyme-mediated PAR2 activity. We compared low-dose trypsin (15 $U \cdot mL^{-1}$)-induced relaxations of mesenteric arteries in C57 and db/db (Figure 7C). Trypsin-induced relaxations of untreated C57 were not significantly different from those in untreated db/db (Bonferroni *post hoc*). In the presence of L-NAME, apamin plus ChTx abolished the trypsin-induced relaxations of mesenteric arteries in both C57 and db/db mice (Figure 7C).

To differentiate between the contributions of BK_{Ca} and SK3.1 to the response, we determined the effects of IbTX and ChTx on ACh-, 2fly- and trypsin-induced relaxations of db/db arteries. ChTx (BK_{Ca} and SK3.1 inhibitor) abolished the residual non-NO-mediated ACh-mediated relaxations (Figure 8A). The BK_{Ca}-selective inhibitor IbTx inhibited ACh-induced relaxations as effectively as ChTx in db/db. In contrast, the attenuation of the 2fly- and trypsin-induced relaxations induced by ChTx was not reproduced by substituting IbTx for ChTx (Figure 8B and C). Trypsin-induced vasodilation was abolished by damaging the endothelium in C57 ($n = 3$) and db/db ($n = 7$; $P > 0.05$, relaxation values were not different than 0, one sample t-test).

Changes in PAR2 expressions in mesenteric artery of db/db mice

PAR2 mRNA expression (normalized to triad housekeeper) was significantly up-regulated in db/db mesenteric arterial

Table 1

Parameters for 2-furoyl-LIGRLO-amide (2fly), ACh and nitroprusside concentration-relaxation response curves in db/db and C57 mesenteric arteries

Drugs	Strain	–log EC_{50}	Hill slope	E_{max} (%)
2fly	C57	8.22 ± 0.12	2.4 ± 0.6	96 ± 1
	db/db	8.03 ± 0.08	2.1 ± 0.3	97 ± 1
ACh	C57	7.23 ± 0.09	1.2 ± 0.1	92 ± 1
	db/db	6.49 ± 0.15[a]	1.1 ± 0.2	72 ± 4[a]
Nitroprusside	C57	8.08 ± 0.17	1.0 ± 0.1	93 ± 1
	db/db	7.20 ± 0.12[a]	1.1 ± 0.2	93 ± 1

Values are mean ± SE for $n = 15$ mice per strain.
Variables were determined by curve fitting data points from cumulative drug concentration–response relationships to four parameter logistic equation.
[a]$P < 0.05$, db/db compared with C57BL/6J (C57), Student's *t*-test for unpaired data.
E_{max}, maximum relaxation response (%) where 100% is the complete reversal of contraction.

Table 2

Effects of L-NAME on 2fly, ACh and nitroprusside concentration-relaxation response curves in db/db and C57BL/6J (C57) mesenteric arteries

Drugs	Strain (*n*)	Treatment	–logEC_{50} (M)	Hill slope	E_{max} (%)
2fly	C57 (9)	Control	8.26 ± 0.12	2.0 ± 0.3	96 ± 1
	C57 (9)	L-NAME	7.94 ± 0.10[a]	1.3 ± 0.2[a]	90 ± 4
	db/db (9)	Control	8.07 ± 0.09	2.3 ± 0.3	98 ± 1
	db/db (9)	L-NAME	7.95 ± 0.11	2.2 ± 0.3	92 ± 3
ACh	C57 (6)	Control	7.13 ± 0.10	1.2 ± 0.2	93 ± 2
	C57 (6)	L-NAME	6.97 ± 0.18	1.6 ± 0.3	52 ± 9[a]
	db/db (6)	Control	6.57 ± 0.18	1.0 ± 0.2	67 ± 6
	db/db (6)	L-NAME	6.57 ± 0.43	1.4 ± 0.3	56 ± 12
Nitroprusside	C57 (6)	Control	7.86 ± 0.33	0.9 ± 0.1	93 ± 2
	C57 (6)	L-NAME	7.69 ± 0.16	1.3 ± 0.4	95 ± 5
	db/db (6)	Control	7.27 ± 0.14	1.3 ± 0.4	90 ± 3
	db/db (6)	L-NAME	7.05 ± 0.24	1.0 ± 0.2	91 ± 6

Values represent mean ± SE for n = number of mice.
Variables were determined by curve fitting data points from cumulative drug concentration–response relationships to four parameter logistic equation.
[a]$P < 0.05$, L-NAME compared with control within strain, two-way ANOVA (strain × artery treatment) followed by Bonferroni *post hoc* test.
E_{max}, maximum relaxation response where 100% is complete reversal of contraction. L-NAME (100 μM, 20 min).

beds (Table 3). On the other hand, mRNA expressions of eNOS and sGC were not significantly different between the two strains (Table 3). Western blots of arterial protein from C57 and db/db assayed with anti-human PAR2 monoclonal antibody (SAM11) (Molino *et al.*, 1997) detected an immunoreactive band with a relative molecular weight corresponding to a positive control for PAR2 in mouse cell line (NIH 3T3) lysate (Figure S1A). The densities of the SAM11-reactive bands (normalized to GAPDH) in C57 were not different from those in db/db (Supporting Information Figure S1B). Further test of the specificity of SAM11 antibody indicated the presence of equivalent immunoreactive bands in arterial protein from PAR2 knockout mice (Supporting Information Figure S1C).

Discussion

The main findings of the present study are that PAR2-mediated vascular smooth muscle relaxations were preserved in small mesenteric arteries of obese type 2 diabetic db/db, even though endothelial NO release and NO responsiveness of vascular smooth muscle were reduced. These findings are novel in that the mechanism underlying the PAR2 resistance

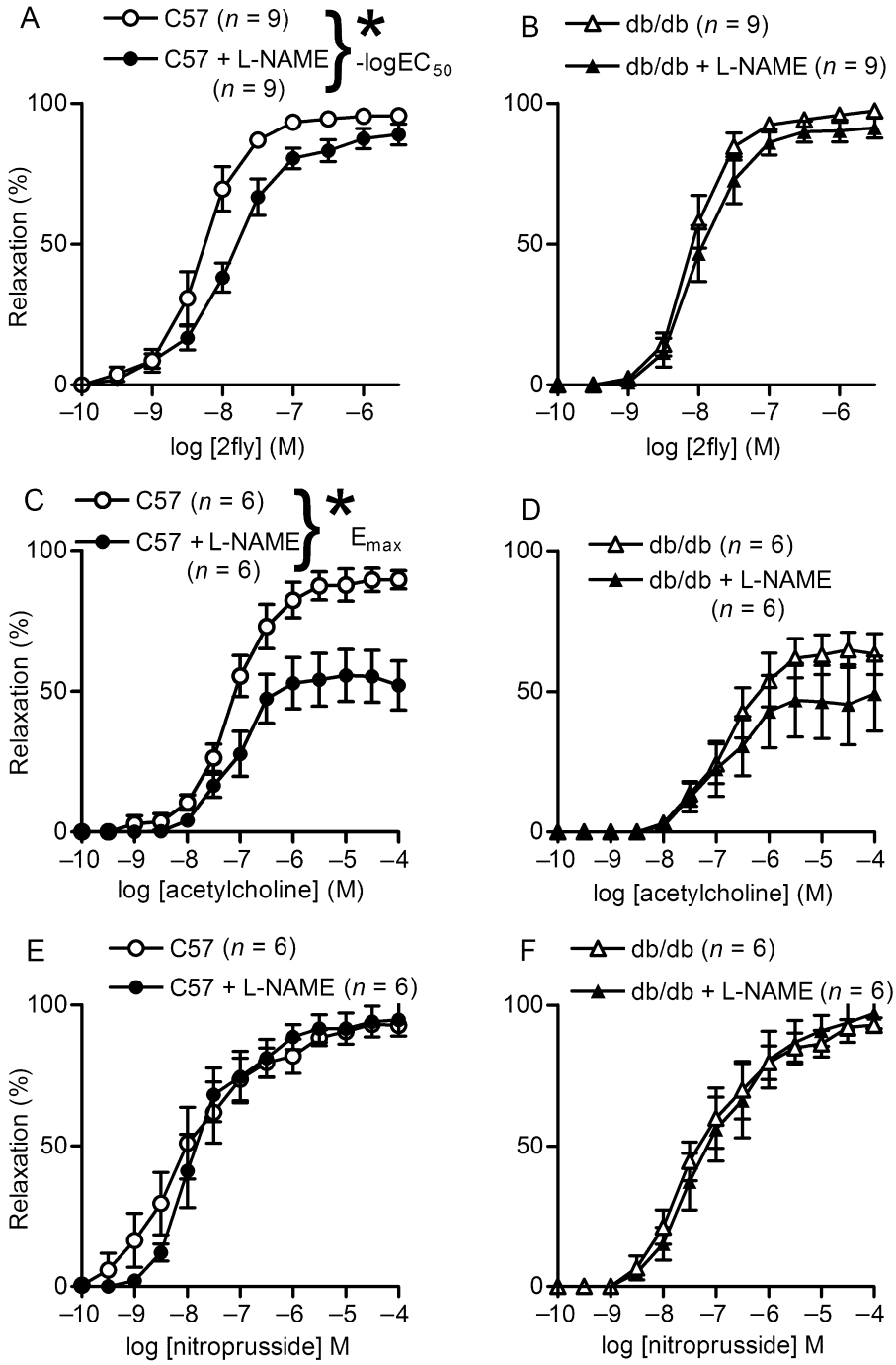

Figure 3

Effects of pretreatment of mesenteric arteries with an inhibitor of NOS on 2-furoyl-LIGRLO-amide (2fly)-, ACh- and nitroprusside-induced relaxations in db/db and C57BL/6J (C57) mice. Values are the mean ± SE (n = number of mice) for (A, B) 2fly- (C, D) ACh-, and nitroprusside (E, F) induced relaxations of C57 and db/db second order mesenteric arteries contracted submaximally by U46619 in the absence or presence of pretreatment with L-NAME (100 μM, 20 min). *$P < 0.05$, C57 untreated (control) compared with L-NAME in (A) –logEC_{50} and hill slope (C) E_{max}, 2-way ANOVA and Bonferroni *post hoc* test.

to diabetic vascular dysfunction is not associated with changes in either the COX or NO pathways, which have been reported in non-obese type 1 diabetic mice and non-obese type 2 diabetic rats. In db/db, the CRC to the PAR2-activating peptide was not significantly different from that in C57 mice (Figure 2), indicating equivalent efficacy for vasodilatation by PAR2 mechanisms. We found that the PAR2-mediated vasodilatation induced by a PAR2-activating peptide and a selective

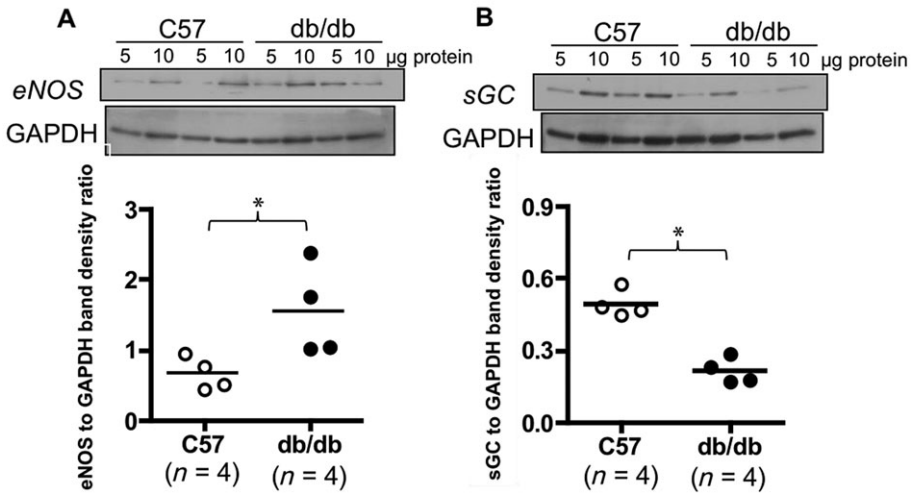

Figure 4

Expression of eNOS and sGC in db/db and C57BL/6J (C57) mesenteric arteries. Upper panels show representative data collected from two db/db and two C57 mice indicating immunoreactive bands corresponding to eNOS and sGC β1 subunit. Each sample was assayed in duplicate at different protein amounts. Lower panels summarize densitometry data collected from four db/db and four C57 mice for eNOS and sGC. Target bands were normalized to the densities of GAPDH bands. *$P < 0.05$, db/db compared with control, Student's *t*-test for unpaired data.

Table 3

mRNA expression of protease-activated receptor 2, endothelial NOS and soluble GC in db/db and C57BL/6J (C57)

mRNA	Ratio (db/db to C57)	SE range
PAR2	1.66[a]	1.09–2.31
eNOS	1.35	0.67–3.18
sGC β1-subunit	1.16	0.71–1.75

mRNA expression in mesenteric arterial cascades was determined by real-time PCR and normalized to a triad housekeeping genes.
db/db, $n = 9$ to 10; C57, $n = 5$ to 6.
SE range: mean minus lower SE to mean plus upper SE.
[a]$P < 0.05$, db/db compared with C57. See Methods for details of statistical analyses.

dose of trypsin (McGuire *et al.*, 2002b) in the db/db mice were endothelium-dependent. If the PAR2-mediated response depends on the same signalling pathways as the endothelial cell-dependent agonist ACh, then the PAR2-mediated actions should have been reduced in db/db mice. An increase in the level of PAR2 mRNA was observed in the mesenteric arteries of db/db compared to C57 mice, which strongly suggests that PAR2 receptor expression was not reduced by obese type 2 diabetes caused by the leptin receptor mutation in db/db. In non-obese diabetic mice (type 1) and type 2 diabetic rats, enhanced PAR2-mediated relaxations and increased mRNA and protein expression in the vascular smooth muscle and endothelium have been reported in large calibre aortas and superior mesenteric arteries, respectively (Roviezzo *et al.*, 2005; Matsumoto *et al.* 2009). Our data together with results obtained from studies in other diabetic models suggest that PAR2-mediated vasodilatations of small- and large-calibre arteries are universally retained independently of the cause or type of diabetes, which differ significantly among the different animal models.

It has been reported that even very brief periods of hyperglycaemia inhibit endothelium-dependent vasodilator activity (Cosentino and Luscher, 1998; Honing *et al.*, 1998); notably, such responses depend on the production and bioavailability of NO. PAR2 activation causes vasodilatation via the production of NO in large-calibre arteries (aortas, femoral arteries) from normal mice (McGuire *et al.*, 2002a). In non-obese type 2 diabetes, increased production of NO from endothelium has been reported as the mechanism underlying the enhanced PAR2-mediated relaxations of superior mesenteric arteries of Goto-Kakizaki rats (Matsumoto *et al.*, 2009). In contrast, it has been shown that decreased bioavailability of NO is involved in the inhibition of endothelium-dependent relaxations to ACh in the small-calibre mesenteric arteries of db/db (Pannirselvam *et al.*, 2002). Therefore, we investigated the possibility that NO contributes to the preservation of PAR2-mediated relaxations in db/db. Indeed, endothelial NO release and NO responsiveness were reduced in db/db small mesenteric arteries. Firstly, we found that the CRC to 2fly was rightward shifted by L-NAME in C57 arteries, but the CRCs were not significantly different between controls and L-NAME treated arteries in db/db. Secondly, we found that the CRCs to nitroprusside were rightward shifted in db/db arteries compared with C57 arteries. An attenuated sensitivity of vascular smooth muscle to nitroprusside has been reported in aortas of db/db (Miike *et al.*, 2008) and ob/ob mice (a model of obesity and type 2 diabetes) (Okon *et al.*, 2003), in aorta and mesenteric artery of rats with obese and type 2 diabetes (Kagota *et al.*, 2006; 2010), and in diabetic patients (Levy *et al.*, 1994). Thirdly, we found that protein expression of eNOS was higher in db/db than in C57, while sGC expression was less in db/db than in C57. These findings

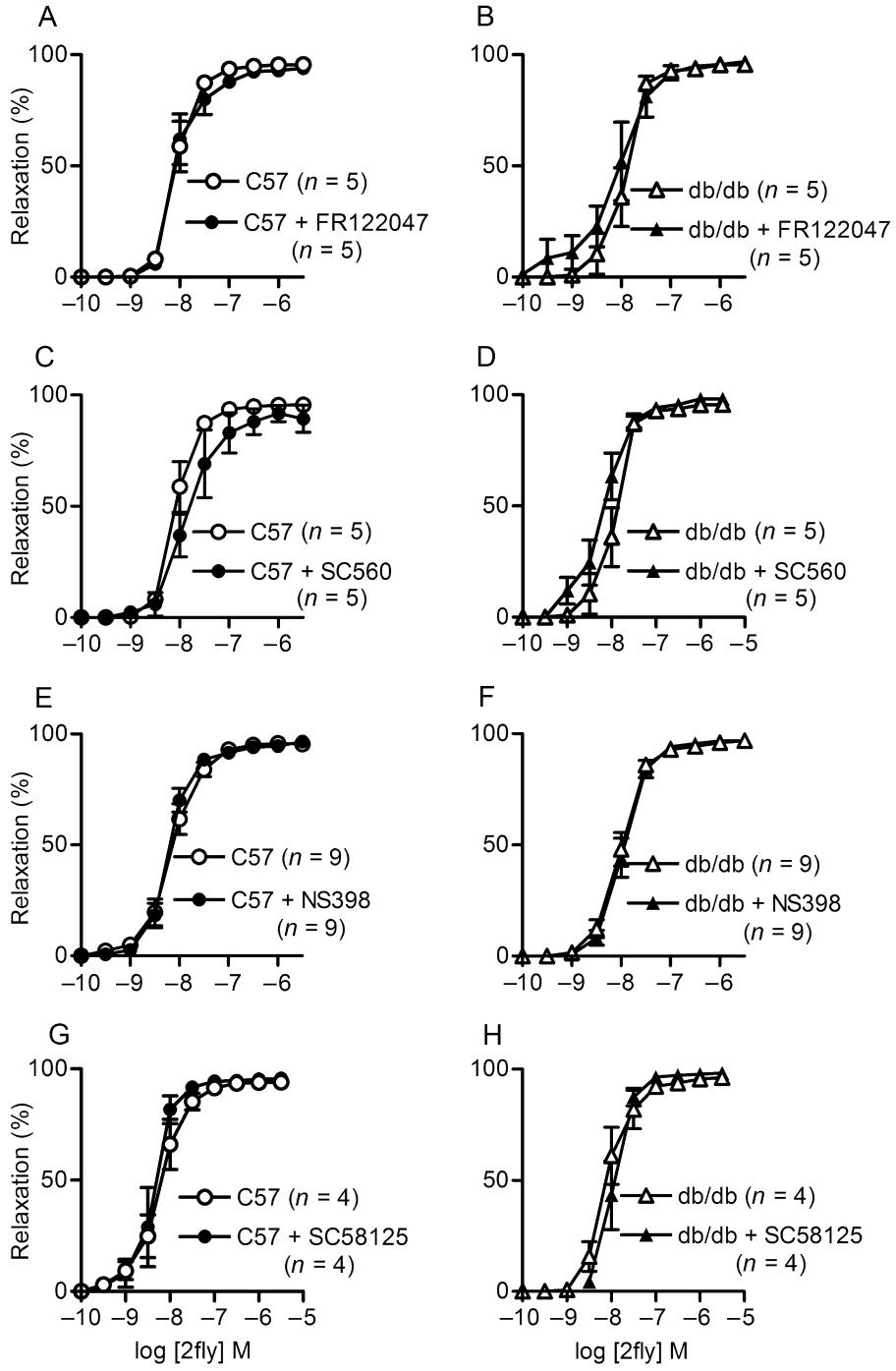

Figure 5

Effects of selective inhibitors of COX-1 (FR122047 and SC560) and -2 (NS398 and SC58125) on 2-furoyl-LIGRLO-amide (2fly)-induced relaxations of db/db and C57BL/6J (C57) mesenteric arteries. Values are the mean ± SE (n = number of mice) for 2fly-induced relaxations of C57 and db/db second order mesenteric arteries contracted submaximally by U46619 in the absence or presence of (A, B) FR122047 (3 μM) (C, D) SC560 (3 μM) (E, F) NS398 (3 μM) and (G, H) SC58125 (10 μM), respectively. Arteries were exposed to inhibitors for 30 min prior to U46619. There were no significant effects of inhibitors or strain on relaxation responses ($P > 0.05$, 2-way ANOVA).

demonstrate that 2fly-induced PAR2-mediated relaxations were preserved even though NO-mediated relaxations were reduced in db/db mesenteric arteries. The simplest interpretation for the deterioration of NO responses would be to attribute it to the lower sGC levels in mesenteric vasculature. However, one possible explanation for the increase in eNOS protein was the presence of more monomeric eNOS in db/db than C57 blood vessels. It has been proposed that monomeric

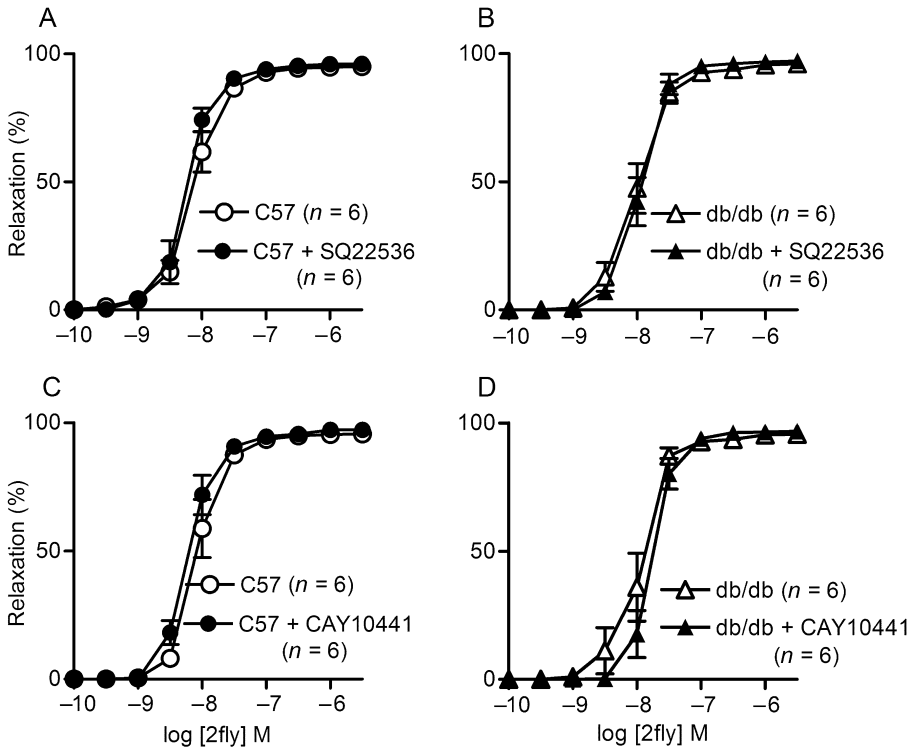

Figure 6

Effects of an AC inhibitor (SQ22536) and PGI_2 receptor antagonist (CAY10441) on 2-furoyl-LIGRLO-amide (2fly)-induced relaxations of db/db and C57BL/6J (C57) mesenteric arteries. Values are the mean ± SE (n = number of mice) for 2fly-induced relaxations of C57 and db/db second order mesenteric arteries contracted submaximally by U46619 in the absence or presence of (A, B) SQ22536 (100 μM) (C, D) CAY10441 (0.3 μM). Arteries were exposed to inhibitors for 30 min prior to U46619. There were no significant effects of inhibitors or strain on relaxation responses ($P > 0.05$, 2-way ANOVA).

eNOS contributes to the inhibition of vasodilator responses by causing an uncoupling of the production of reactive oxygen species. Nevertheless, in db/db, the NO pathway was not functioning the same as in C57, thus this mechanism is unlikely to underlie the preserved PAR2-mediated relaxations.

COX regulates vascular tone via the production of prostaglandins, and an up-regulation of mRNA/protein expression of COX, particularly COX-2, in vascular walls has been shown in experimental models and in humans with diabetes (Guo *et al.*, 2005; Roviezzo *et al.*, 2005; Szerafin *et al.* 2006; Nacci *et al.* 2009). However, there is still controversy regarding the significance of their role in the dysfunctional vascular response occurring in diabetes. For example, increased expression of COX in aortic smooth muscle contributes to enhanced contractions to 5-HT, angiotensin II, phenylephrine and high potassium in db/db type 2 diabetic mice (Guo *et al.*, 2005). However, we found that the contractions to high potassium, U46619 and phenylephrine were unchanged in db/db mesenteric arteries. On the other hand, streptozotocin-induced type 1 diabetic mice show an increased endothelial COX-2 expression, and this up-regulation is a compensatory response that opposes the endothelial dysfunction (Nacci *et al.*, 2009). Furthermore, increased COX-2 expression in aortic smooth muscle has been associated with the mechanism underlying enhanced PAR2-mediated relaxations in NOD mice (Roviezzo *et al.*, 2005). Therefore, to test the contribution of COX pathway in preserving PAR2-mediated relaxations in db/db, we determined the protein expressions of COX-1 and COX-2, and the effects of their selective inhibitors on PAR2-mediated relaxations of mesenteric arteries. Contrary to the findings in other diabetic animals, neither COX-1 nor COX-2 expression were significantly different between db/db and C57, and the CRCs to 2fly were not significantly different in the presence or absence of the selective COX-1, COX-2, AC inhibitors and PGI_2 receptor antagonist in db/db. Thus, we conclude that the mechanism underlying PAR2 resistance to diabetic vascular dysfunction is not linked to the COX-cAMP pathway in db/db.

In various resistance arteries, which include middle cerebral and second order mesenteric arteries, PAR2 mediates vasodilatation by inducing a non-NO non-COX-mediated endothelium-dependent hyperpolarization (EDH) of vascular smooth muscle (McGuire *et al.*, 2002b; 2004; Smeda and McGuire, 2007; Smeda *et al.* 2010). Evidence of some compensatory increases in such non-NO mechanisms has been obtained in mesenteric and coronary arteries of db/db (Pannirselvam *et al.*, 2002; 2006; Park *et al.*, 2008). Of particular importance to our study are the observations that IbTx or ChTx alone were able to block ACh-induced EDH relaxations of db/db mesenteric arteries (Pannirselvam *et al.*, 2006). We reproduced those findings (Figure 8A) and tested the

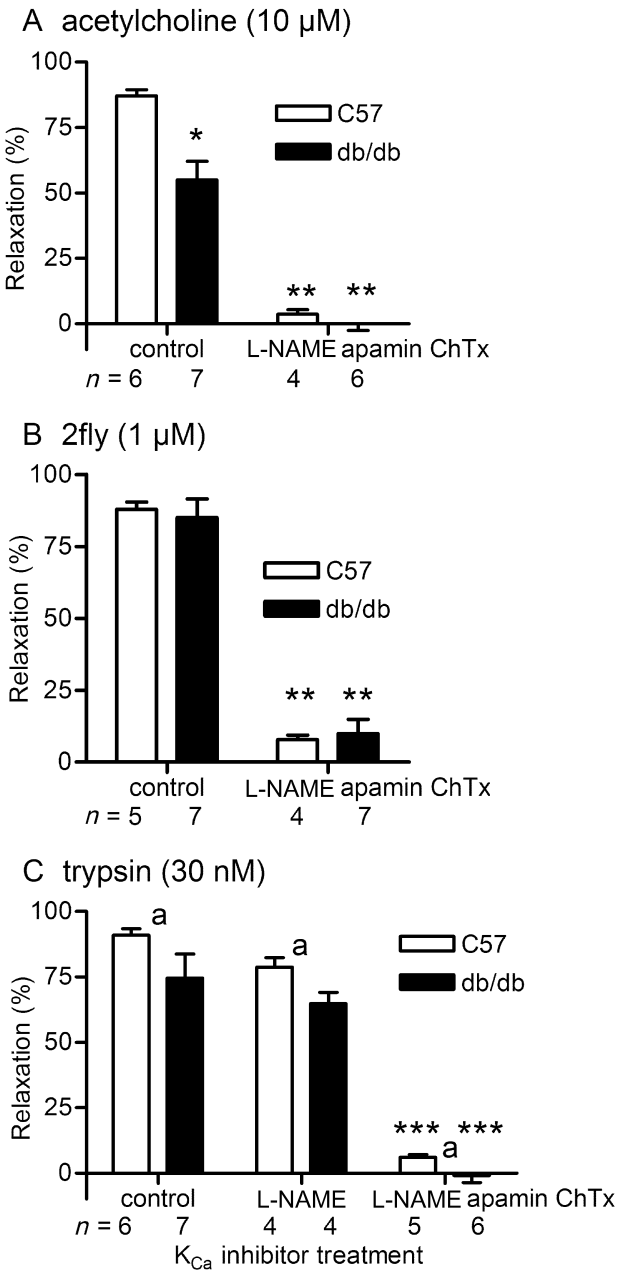

Figure 7

Effects of K_{Ca} inhibition by apamin + charybdotoxin on ACh, 2-furoyl-LIGRLO-amide (2fly)- and trypsin-induced relaxations of db/db and C57BL/6J (C57) mesenteric arteries. Columns are the mean ± SE (n = number of mice) for (A) ACh- (B) 2fly- and (C) trypsin-induced relaxations of C57 and db/db second order mesenteric arteries contracted submaximally by U46619. Arteries were exposed to inhibitors [100 μM L-NAME, 1 μM apamin, 50 nM charybdotoxin (ChTx)] for 30 min prior to U46619. *P < 0.05, compared with C57 control (untreated); **P < 0.05, compared with same strain control (untreated); ***P < 0.05, compared with same strain control (untreated) and same strain L-NAME-treated, two-way ANOVA (strain × treatment) and Bonferroni *post hoc*. [a] P < 0.05, main effect of strain contributed 2.5% of total variation, two-way ANOVA. In (C) control C57 vs. control db/db, and control db/db vs. L-NAME-treated db/db were not different, Bonferroni *post hoc*. In (B) and (C), the interaction between strain and treatment was not significant (P > 0.05).

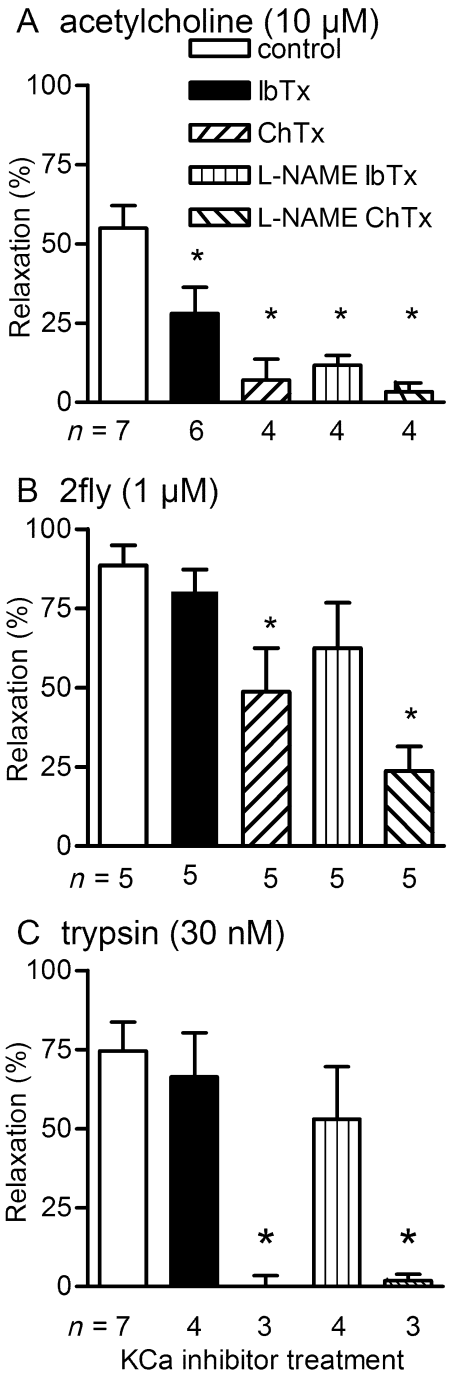

Figure 8

Effects of iberiotoxin (IbTx) and charybdotoxin (ChTx) on ACh, 2-furoyl-LIGRLO-amide (2fly)- and trypsin-induced relaxations of db/db mesenteric arteries. Columns are the mean ± SE (n = number of mice) for (A) ACh- (B) 2fly- and (C) trypsin-induced relaxations of db/db second order mesenteric arteries contracted submaximally by U46619. Arteries were exposed to inhibitors (100 μM L-NAME, 50 nM IbTx, 50 nM ChTx) for 30 min prior to U46619. *P < 0.05, compared with control (untreated) 1 way ANOVA and Bonferroni *post hoc*.

contributions of K_{Ca} to PAR2 activity in db/db (Figures 7 and 8). Based on the inhibition by ChTx, but not by IbTx, we conclude that both the enzyme- and PAR2-activating peptide-mediated relaxations are produced primarily via activation of SK3.1 in db/db (Figure 8B and C). The PAR2-mediated relaxations induced by 2fly and trypsin were endothelium-dependent in db/db. Thus, an endothelium-derived hyperpolarizing response via SK3.1 contributes to the retention of the PAR2-mediated relaxation in mesenteric artery of db/db.

An additional explanation for the preservation of the 2fly-induced relaxation is that PAR2 expression is changed in db/db. We found a higher level of PAR2 mRNA in mesenteric arteries of db/db, but we did not find any differences in PAR2 protein expression. However, our data show that the monoclonal antibody SAM11, which was raised against the tethered ligand of human PAR2 (Molino *et al.*, 1997), is cross-reactive with an unknown target in arterial protein isolated from PAR2-knockout mice. This creates uncertainty about the application of this antibody in Western blots to measure PAR2 protein in rodent vascular tissue (Aman *et al.*, 2010). Although the relaxation activity of PAR2 was found to be endothelium-dependent in mesenteric arteries of db/db, this does not exclude the possibility of changes in vascular smooth muscle PAR2 expression occurring in these mice. Where and how PAR2 is expressed in mesenteric arteries of db/db remains unknown. An up-regulation of PAR2 expression by pro-inflammatory cytokines and agents, for example IL-1β, TNF-α and LPS, has been demonstrated in both *in vitro* and *in vivo* studies (Cicala *et al.* 1999; Hamilton *et al.*, 2001). Chronic low-grade inflammation may be a condition linking the occurrence of excessive amounts of adipose tissue to obesity-associated pathologies such as type 2 diabetes and cardiovascular diseases. Adipose tissue produces leptin, angiotensinogen, TNF-α, IL-6 and monocyte chemoattractant protein-1, which all have the ability to contribute to vascular inflammation (Dandona *et al.* 2005; Paoletti *et al.*, 2006; Zhang and Zhang, 2009; Ikeoka *et al.* 2010). These observations lead to a novel hypothesis that the inflammatory adipokines contribute to the up-regulation of PAR2 in arteries of db/db mice. Further studies are needed to define the mechanisms and the pathophysiological significance of the PAR2 gene regulation changes in db/db.

In conclusion, PAR2-mediated relaxations were protected from vascular dysfunction in db/db. SK3.1 activation was the primary mechanism for the PAR2-mediated vasodilatation in db/db. Our findings indicate that the COX and/or NO pathway do not contribute to the PAR2-mediated relaxations in obese type 2 diabetic db/db. Preserved vascular PAR2 activity and increased expression may be linked to cardiovascular inflammation caused by obesity under conditions of type 2 diabetes.

Acknowledgements

The authors thank Keon Hughes, Dr J Dore, Dr JL Vanderluit, Dr M. Woods and Dr S Vasdev for their helpful advice and use of laboratory equipment at Memorial University. These studies were funded by operating and infrastructure grants to JJM from the Canadian Institutes of Health Research (CIHR: ROP-88065; CIHR New Investigator: RSH-78370) and the Research and Development Corporation of Newfoundland and Labrador (IRIF: 0708–022, 0708–008).

Conflict of Interest

The authors declare no conflict of interests.

References

Aman M, Hirano M, Kanaide H, Hirano K (2010). Upregulation of proteinase-activated receptor-2 and increased response to trypsin in endothelial cells after exposure to oxidative stress in rat aortas. J Vasc Res 47: 494–506.

Belmadani S, Palen DI, Gonzalez-Villalobos RA, Boulares HA, Matrougui K (2008). Elevated epidermal growth factor receptor phosphorylation induces resistance artery dysfunction in diabetic db/db mice. Diabetes 57: 1629–1637.

Cao J, Kitazawa T, Takehana K, Taneike T (2006). Endogenous prostaglandins regulate spontaneous contractile activity of uterine strips isolated from non-pregnant pigs. Prostaglandins Other Lipid Mediat 81: 93–105.

Cicala C, Pinto A, Bucci M, Sorrentino R, Walker B, Harriot P *et al.* (1999). Protease-activated receptor-2 involvement in hypotension in normal and endotoxemic rats in vivo. Circulation 99: 2590–2597.

Cosentino F, Luscher TF (1998). Endothelial dysfunction in diabetes mellitus. J Cardiovasc Pharmacol 32 (Suppl. 3): S54–S61.

Damiano BP, D'Andrea MR, de Garavilla L, Cheung WM, Andrade-Gordon P (1999). Increased expression of protease activated receptor-2 (PAR-2) in balloon-injured rat carotid artery. Thromb Haemost 81: 808–814.

Dandona P, Aljada A, Chaudhuri A, Mohanty P, Garg R (2005). Metabolic syndrome: a comprehensive perspective based on interactions between obesity, diabetes, and inflammation. Circulation 111: 1448–1454.

Guo Z, Su W, Allen S, Pang H, Daugherty A, Smart E *et al.* (2005). COX-2 up-regulation and vascular smooth muscle contractile hyperreactivity in spontaneous diabetic db/db mice. Cardiovasc Res 67: 723–735.

Hamilton JR, Frauman AG, Cocks TM (2001). Increased expression of protease-activated receptor-2 (PAR2) and PAR4 in human coronary artery by inflammatory stimuli unveils endothelium-dependent relaxations to PAR2 and PAR4 agonists. Circ Res 89: 92–98.

Hansen KK, Oikonomopoulou K, Li Y, Hollenberg MD (2008). Proteinases, proteinase-activated receptors (PARs) and the pathophysiology of cancer and diseases of the cardiovascular, musculoskeletal, nervous and gastrointestinal systems. Naunyn Schmiedebergs Arch Pharmacol 377: 377–392.

Honing ML, Morrison PJ, Banga JD, Stroes ES, Rabelink TJ (1998). Nitric oxide availability in diabetes mellitus. Diabetes Metab Rev 14: 241–249.

Ikeoka D, Pachler C, Korsatko S, Mader JK, Weinhandl H, Bodenlenz M *et al.* (2010). Interleukin-6 produced in subcutaneous

adipose tissue is linked to blood pressure control in septic patients. Cytokine 50: 284–291.

Kagota S, Yamaguchi Y, Tanaka N, Kubota Y, Kobayashi K, Nejime N *et al*. (2006). Disturbances in nitric oxide/cyclic guanosine monophosphate system in SHR/NDmcr-cp rats, a model of metabolic syndrome. Life Sci 78: 1187–1196.

Kagota S, Fukushima K, Umetani K, Tada Y, Nejime N, Nakamura K *et al*. (2010). Coronary vascular dysfunction promoted by oxidative-nitrative stress in SHRSP.Z-Lepr(fa) /IzmDmcr rats with metabolic syndrome. Clin Exp Pharmacol Physiol 37: 1035–1043.

Kennedy AJ, Ellacott KL, King VL, Hasty AH (2010). Mouse models of the metabolic syndrome. Dis Model Mech 3: 156–166.

Levy J, Gavin JR, III, Sowers JR (1994). Diabetes mellitus: a disease of abnormal cellular calcium metabolism? Am J Med 96: 260–273.

McGuire JJ, Dai J, Andrade-Gordon P, Triggle CR, Hollenberg MD (2002a). Proteinase-activated receptor-2 (PAR2): vascular effects of a PAR2-derived activating peptide via a receptor different than PAR2. J Pharmacol Exp Ther 303: 985–992.

McGuire JJ, Hollenberg MD, Andrade-Gordon P, Triggle CR (2002b). Multiple mechanisms of vascular smooth muscle relaxation by the activation of proteinase-activated receptor 2 in mouse mesenteric arterioles. Br J Pharmacol 135: 155–169.

McGuire JJ, Hollenberg MD, Bennett BM, Triggle CR (2004). Hyperpolarization of murine small caliber mesenteric arteries by activation of endothelial proteinase-activated receptor 2. Can J Physiol Pharmacol 82: 1103–1112.

McGuire JJ, Van Vliet BN, Gimenez J, King JC, Halfyard SJ (2007). Persistence of PAR-2 vasodilation despite endothelial dysfunction in BPH/2 hypertensive mice. Pflugers Arch 454: 535–543.

Matsumoto T, Ishida K, Taguchi K, Kobayashi T, Kamata K (2009). Mechanisms underlying enhanced vasorelaxant response to protease-activated receptor 2-activating peptide in type 2 diabetic Goto-Kakizaki rat mesenteric artery. Peptides 30: 1729–1734.

Miike T, Kunishiro K, Kanda M, Azukizawa S, Kurahashi K, Shirahase H (2008). Impairment of endothelium-dependent ACh-induced relaxation in aorta of diabetic db/db mice–possible dysfunction of receptor and/or receptor-G protein coupling. Naunyn Schmiedebergs Arch Pharmacol 377: 401–410.

Molino M, Barnathan ES, Numerof R, Clark J, Dreyer M, Cumashi A *et al*. (1997). Interactions of mast cell tryptase with thrombin receptors and PAR-2. J Biol Chem 272: 4043–4049.

Nacci C, Tarquinio M, De BL, Mauro A, Zigrino A, Carratu MR *et al*. (2009). Endothelial dysfunction in mice with streptozotocin-induced type 1 diabetes is opposed by compensatory overexpression of cyclooxygenase-2 in the vasculature. Endocrinology 150: 849–861.

Napoli C, de Nigris F, Wallace JL, Hollenberg MD, Tajana G, De Rosa G *et al*. (2004). Evidence that protease activated receptor 2 expression is enhanced in human coronary atherosclerotic lesions. J Clin Pathol 57: 513–516.

Okon EB, Szado T, Laher I, McManus B, van Breemen C (2003). Augmented contractile response of vascular smooth muscle in a diabetic mouse model. J Vasc Res 40: 520–530.

Pannirselvam M, Verma S, Anderson TJ, Triggle CR (2002). Cellular basis of endothelial dysfunction in small mesenteric arteries from spontaneously diabetic (db/db -/-) mice: role of decreased tetrahydrobiopterin bioavailability. Br J Pharmacol 136: 255–263.

Pannirselvam M, Ding H, Anderson TJ, Triggle CR (2006). Pharmacological characteristics of endothelium-derived hyperpolarizing factor-mediated relaxation of small mesenteric arteries from db/db mice. Eur J Pharmacol 551: 98–107.

Paoletti R, Bolego C, Poli A, Cignarella A (2006). Metabolic syndrome, inflammation and atherosclerosis. Vasc Health Risk Manag 2: 145–152.

Park Y, Capobianco S, Gao X, Falck JR, Dellsperger KC, Zhang C (2008). Role of EDHF in type 2 diabetes-induced endothelial dysfunction. Am J Physiol Heart Circ Physiol 295: H1982–H1988.

Pfaffl MW, Horgan GW, Dempfle L (2002). Relative expression software tool (REST) for group-wise comparison and statistical analysis of relative expression results in real-time PCR. Nucleic Acids Res 30: e36.

Ramachandran R, Hollenberg MD (2008). Proteinases and signalling: pathophysiological and therapeutic implications via PARs and more. Br J Pharmacol 153 (Suppl. 1): S263–S282.

Roviezzo F, Bucci M, Brancaleone V, Di LA, Geppetti P, Farneti S *et al*. (2005). Proteinase-activated receptor-2 mediates arterial vasodilation in diabetes. Arterioscler Thromb Vasc Biol 25: 2349–2354.

Russell JC, Proctor SD (2006). Small animal models of cardiovascular disease: tools for the study of the roles of metabolic syndrome, dyslipidemia, and atherosclerosis. Cardiovasc Pathol 15: 318–330.

Shaw DI, Hall WL, Williams CM (2005). Metabolic syndrome: what is it and what are the implications? Proc Nutr Soc 64: 349–357.

Smeda JS, McGuire JJ (2007). Effects of poststroke Losartan versus Captopril treatment on myogenic and endothelial function in the cerebrovasculature of SHRsp. Stroke 38: 1590–1596.

Smeda JS, McGuire JJ, Daneshtalab N (2010). Protease-activated receptor 2 and bradykinin-mediated vasodilation in the cerebral arteries of stroke-prone rats. Peptides 31: 227–237.

Sobey CG, Cocks TM (1998). Activation of protease-activated receptor-2 (PAR-2) elicits nitric oxide-dependent dilatation of the basilar artery in vivo. Stroke 29: 1439–1444.

Szerafin T, Erdei N, Fulop T, Pasztor ET, Edes I, Koller A *et al*. (2006). Increased cyclooxygenase-2 expression and prostaglandin-mediated dilation in coronary arterioles of patients with diabetes mellitus. Circ Res 99: e12–e17.

Venkatapuram S, Shannon RP (2006). Managing atherosclerosis in patients with type 2 diabetes mellitus and metabolic syndrome. Am J Ther 13: 64–71.

Yamada Y, Yamauchi D, Yokoo M, Ohinata K, Usui H, Yoshikawa M (2008). A potent hypotensive peptide, novokinin, induces relaxation by AT2- and IP-receptor-dependent mechanism in the mesenteric artery from SHRs. Biosci Biotechnol Biochem 72: 257–259.

Zhang H, Zhang C (2009). Regulation of microvascular function by adipose tissue in obesity and type 2 diabetes: evidence of an adipose-vascular loop. Am J Biomed Sci 1: 133–142.

Supporting information

Additional Supporting Information may be found in the online version of this article:

Figure S1 Monoclonal antibody SAM-11 immunoreactivity in mesenteric arterial protein from C57, db/db and PAR2 knockout mice**.** (A) Immunoreactive bands corresponding to PAR_2 in mesenteric arterial protein collected from four C57 and four db/db mice. NIH3T3 cell lysate provided by supplier (Santa Cruz, CA, USA) was included as a positive control for PAR_2 immunoreactivity. (B) Summarized densitometry data for the SAM11-target bands in C57 and db/db shown in (A). (C) Representative SAM-11 (1:3000) immunoblotting data collected from one C57 and one PAR_2 knockout ($PAR_2^{-/-}$) mouse. C57 sample was assayed in duplicate at two protein amounts. In (A) and (C), L indicates the lane containing the molecular weight ladders; values (kDa) of the relative molecular weight standards are included in (C). Target bands were normalized to the densities of GAPDH bands. $P > 0.05$, db/db compared with control Student's *t*-test for unpaired data.

Table S1 Compiled gene and protein target sequence data for TaqMan gene expression assay

Please note: Wiley-Blackwell are not responsible for the content or functionality of any supporting materials supplied by the authors. Any queries (other than missing material) should be directed to the corresponding author for the article.